JOURNAL OF COMPUTATIONAL PHYSICS 70, 218–231 (1987)

An Efficient Algorithm for Solving the Vibronic Coupling Problem

K. P. LAWLEY

Department of Chemistry, University of Edinburgh, West Mains Road, Edinburgh EH9 3JJ, United Kingdom

Received December 31, 1985; revised August 4, 1986

The two state coupling problem in wave mechanics is solved in discretized form using the sign changes in the Sturm sequence of the Hamiltonian λ-determinant. The numerical algorithm is simple and fast; precision and accuracy can be separately controlled. The method is applied to the vibronic coupling problem in a diatomic (two closed channels) and the evolution of the adiabatic vibronic levels from the uncoupled (diabatic) states is demonstrated as a function of the strength of coupling. The method can be used for any symmetric pentadiagonal band matrix eigenvalue problem. © 1987 Academic Press, Inc.

INTRODUCTION

The higher vibronic levels of molecules are generally embedded in a manifold of levels belonging to neighbouring states. Symmetry permitting, these electronic states are coupled (e.g., by the spin orbit operator) and the wave equation is no longer strictly separable into vibrational and electronic factors. The problem is already present in diatomic and leads, for instance, to the mixing of Rydberg with ion pair states and to predissociation.

The simplest and most common problem is that of two interacting electronic states. Writing the complete vibronic wave function thus,

$$\Psi_n = \psi_1^{(e)}(r)\,\phi_{1n}(x) + \psi_2^{(e)}(r)\,\phi_{2n}(x), \tag{1}$$

where $\psi_1^{(e)}(r)$ and $\psi_2^{(e)}(r)$ are the electronic eigenfunctions of the unmixed (i.e., diabatic) states (r is a collective electronic coordinate), the vibrational wave functions ϕ_{1n} and ϕ_{2n} satisfy the standard coupled wave equations

$$\begin{aligned}[(-\hbar^2/2\mu)\,d^2/dx^2 + V_{11}(x) - E_n]\,\phi_{1n}(x) &= V_{12}(x)\,\phi_{2n}(x)\\ [(-\hbar^2/2\mu)\,d^2/dx^2 + V_{22}(x) - E_n]\,\phi_{2n}(x) &= V_{21}(x)\,\phi_{1n}(x),\end{aligned} \tag{2}$$

where $V_{11}(x)$, $V_{22}(x)$ are the diabatic potential energy functions for the nuclear motion and where V_{12} is the coupling matrix element in the diabatic basis. The alternative formulation of the coupling problem in the adiabatic basis leads to the

0021-9991/87 $3.00

operator d/dx appearing on the right-hand side of (2). The eigenvalues of these coupled equations can also be found by the method to be presented and the algorithm is given in Appendix C.

Equations (2) (or those in the adiabatic basis) have hitherto been solved numerically either by expanding the ϕ_i in soma appropriate set of basis functions and diagonalising the resultant H matrix, or by employing a finite difference stepwise integration procedure. Our method is also a finite difference one, although integration is not used.

If the eigenfunctions are tabulated at N equally spaced intervals $\xi = (x_i - x_{i-1})$ and d^2/dx^2 replaced by the second central difference $\delta_i^{(2)}$ at each tabulation position, we obtain $2N$ simultaneous equations

$$\begin{aligned}[\delta_i^{(2)} - 2\mu\,\xi^2/\hbar^2(V_{11}(x_i) - E)]\,\phi_1(x_i) &= 2\mu\xi^2/\hbar^2 V_{12}(x_1)\,\phi_2(x_i)\\ [\delta_i^{(2)} - 2\mu\,\xi^2/\hbar^2(V_{22}(x_i) - E)]\,\phi_2(x_i) &= 2\mu\xi^2/\hbar^2 V_{21}(x_i)\,\phi_1(x_i),\end{aligned} \tag{3}$$

where the correction term $O(\xi^4\phi^{iv})$ has been omitted. Introducing the reduced functions

$$W_i^{nn'} = 2\mu\xi^2/\hbar^2\, V_{nn'}(x_i); \qquad \lambda = 2\mu\xi^2 E/\hbar^2 \tag{4}$$

the problem is reduced to finding the eigenvalues λ_n of a Hamiltonian matrix whose structure is much simpler than that encountered in a functional expansion, though its dimension is considerably larger.

For the uncoupled one channel problem ($V_{12} = 0$) this leads [1, 2] to a tridiagonal Hamiltonian matrix

$$\begin{bmatrix} W_1+2-\lambda & -1 & 0 & \cdot & \cdot & 0 \\ -1 & W_2+2-\lambda & -1 & 0 & & \cdot \\ 0 & -1 & W_3+2-\lambda & -1 & & \cdot \\ \cdot & & \cdot & \cdot & & \cdot \\ \cdot & & & & \cdot & -1 \\ 0 & \cdot & \cdot & & -1 & W_N+2-\lambda \end{bmatrix} \tag{5}$$

and for the coupled equations (3) the discretized Hamiltonian $\mathbf{H} - \lambda\mathbf{I}$ matrix is pentadiagonal

$$\left[\begin{array}{cc|c|cc|c} W_1''+2-\lambda & W_1^{12} & -1 & 0 & \cdot & 0 \\ \hline W_1^{12} & W_1^{22}+2-\lambda & 0 & -1 & \cdot & \cdot \\ \hline -1 & 0 & W_2^{11}+2-\lambda & W_2^{12} & -1 & \cdot \\ \hline 0 & -1 & W_2^{12} & W_2^{22}+2-\lambda & 0 & \cdot \\ \cdot & \cdot & \cdot & \cdot & \cdot & W_N^{12} \\ 0 & \cdot & \cdot & -1 & W_N^{12} & W_N^{22}+2-\lambda \end{array}\right] \tag{6}$$

Note that the eigenvector consists of alternate contributions from the two parts of the composite wave function. It is the purpose of this paper to show that the roots of (6) can be found rapidly from a Sturm sequence. Currently used stepwise integration procedures [3, 4] start from the Numerov formulation in which the correction term $O(\xi^4)$ is replaced by one $O(\xi^6\phi^{vi})$. Forward and backward integration is then used starting from orthogonal boundary conditions (5) followed by a matching procedure to ensure continuity of the two solution vectors. The Numerov procedure can be incorporated into the matrix from (6), resulting in a 7-diagonal matrix. Partly because of the increased width of the diagonal band, but also because of the danger of poor behaviour of the Numerov procedure in problems involving tunnelling, we have retained the simpler second difference formulation. The price paid is, of course, that root convergence is now only quadratic in the step length as opposed to the ξ^4 convergence achieved by Numerov based methods. However, we contend that the speed and stability of the method make extrapolation very fast if the highest accuracy is required.

A further advantage of retaining the form (6) is that minimal changed are required if the coupling operator is switched to d/dx. Under those conditions the Numerov procedure would not be applicable.

2. The Numerical Algorithm

Bisecting the λ-determinant is the preferred method [5] for finding the roots of a tridiagonal matrix and we now show that the method can be applied to a pentadiagonal matrix. Essentially, a trial value of root is selected and the number, n, of sign changes in the Sturm sequence of principal minor determinants of increasing order down the leading diagonal is counted. The fact that this sequence forms a Sturm sequence if the complete determinant is symmetric is proved in Ref. [6]. These minor determinants, $\Delta^{(i)}$ are defined by the dotted lines in the matrix (6). The number of eigenvalues with energy $<\lambda$ is then equal to n. A moment's consideration shows that all that is required is the number of negative values in the sequence of the ratios of successive minors, and this is the basis of the standard bisection algorithm for tridiagonal matrices, in which successive trial values of the Kth root are the arithmetic average of the previous upper and lower limits to E_K.

Consider the pentadiagonal determinant

$$\Delta^N(\lambda)=\begin{vmatrix} d_1-\lambda & e_2 & f_3 & 0 & 0 & \cdot \\ e_2 & d_2-\lambda & e_3 & f_4 & 0 & \cdot \\ f_3 & e_3 & d_3-\lambda & e_4 & f_5 & \cdot \\ 0 & & \cdot & & & \\ \cdot & & & \cdot & & \\ \cdot & & & & & \cdot \\ 0\cdots f_u & e_N & \cdot & f_N & e_N & d-\lambda \end{vmatrix}, \tag{7}$$

where the non-standard notation for matrix elements has been used because, in manipulating the determinant, the various entries will be drawn from linear arrays $\{d\}$, $\{e\}$, etc., rather than from a square matrix.

The sequence of minor determinants of increasing order, $\Delta^{(i)}$ starting at the upper left entry is

$$\Delta^{(0)}=1, \quad \Delta^{(1)}=d_1-\lambda, \qquad \Delta^{(2)}=(d_1-\lambda)(d_2-\lambda)-e_2^2,\ldots. \tag{8}$$

Let the minor of $\Delta^{(i)}$, obtained by deleting the nth row and mth column be $\Delta^{(i)}_{nm}$ (so $\Delta^{(i)}_{ii}=\Delta^{(i-1)}$). We require the number of sign changes of $\Delta^{(i)}$ in passing from $i=1$ to N as counted by negative values of the ratio $\Delta^{(i)}/\Delta^{(i-1)}$. For this we generate the following recursive sequence from the elementary properties of determinants,

$$\begin{aligned}
\Delta^{(i)} &= (d_i-\lambda)\,\Delta^{(i-1)}-e_i\Delta^{(i)}_{i,i-1}+f_i\Delta^{(i)}_{i,i-2}\\
\Delta^{(i)}_{i,i-1} &= e_i\Delta^{(i-2)}-f_i\Delta^{(i-1)}_{i-1,i-2}\\
\Delta^{(i)}_{i,i-2} &= e_i\Delta^{(i-1)}_{i-1,i-2}-f_i\Delta^{(i-1)}_{i-2,i-2}\\
\Delta^{(i)}_{i-1,i-1} &= (d_i-\lambda)\,\Delta^{(i-2)}-f_i^2\Delta^{(i-3)},
\end{aligned} \tag{9}$$

and it is upon this sequence that the present algorithm is based. The application of the method to the matrix (6) is speeded up by the alternate zeros in $\{e\}$ and the actual algorithms given in appendix (1). For comparison, the sequence for a trigiagonal matrix is of only two steps: (f bands omitted),

$$\begin{aligned}
\Delta^{(i)} &= (d_i-\lambda)\,\Delta^{(i-1)}-e_i\Delta^{(i)}_{i,i-1}\\
\Delta^{(i)}_{i,i-1} &= e_i\Delta^{(i-2)}.
\end{aligned} \tag{10}$$

Typically, for the lower lying vibrational levels ($v<50$) N between 800 and 1200 gives eigenvalues to 1 part in 10^4 or better. This value of N represents a step length of between 0.002 and 0.001 Å, and in order to maintain this steplength for high vibrational levels of correspondingly large amplitude of vibration, N may have to be increased to perhaps 5000. A key parameter from the computational point of view is the precision η to which roots are found. The number of passes through the sequence that is needed increases as $-\ln\eta$. Bisection becomes inefficient if the highest accuracy is required and Newton Raphson interpolation on the full determinant $\Delta^{(N)}(\lambda)$ should then be used (see Appendix A). Naturally, η must be set to a value less than the smallest separation between roots. True degeneracy, as opposed to accidental, can be handled by transforming to a symmetry adapted coordinate basis. It can readily be shown that, if there is n-fold degeneracy of a given root, the last n principal minors, $\Delta^{(N)}(\lambda),\ldots, \Delta^{(N-n+1)}(\lambda)$ are zero.

We emphasise that the sequence of minors $\Delta^{(1)}$, $\Delta^{(2)},\ldots, \Delta^{(N)}$ does not constitute a wave function. Although the resemblance is quite close in the tridiagonal (single channel) case, the $\Delta^{(i)}$ do not satisfy the finite difference equations (3). If eigenvec-

tors are required (and almost any problem in wave mechanics can be formulated in terms of eigenvalues rather than eigenfunctions) they are produced by one or two cycles of back substitution just as in the single channel case.

4. Convergence with Decreasing Step Length, ξ

To achieve the highest accuracy, extrapolation to $\xi = 0$ must be used, and we now illustrate the strict quadratic dependence of $\lambda_n(\xi)$. $V_{11}(x)$ and $V_{22}(x)$ are assumed parabolic and the coupling is exponential

$$V_{11}(x),\ V_{22}(x) = k(x(1.5 \pm \delta))^2; \qquad V_{12}(x) = V_{12} \exp(-(x-1.5)/10). \quad (11)$$

The parameter values used were; $\mu = 40$ amu, $k = 40{,}000\ \text{cm}^{-1}\ \text{Å}^2$, $\delta = 0.5$ Å, $V_{12} = 10^3\ \text{cm}^{-1}$ (leading to a crossing of V_{11} and V_{22} at $5000\ \text{cm}^{-1}$, where $V_{12} = 1000\ \text{cm}^{-1}$.) The potentials are sketched in Fig. 1. The interval for x was generally [0, 3] (see note following Table I) and eigenvalues changed by less than $5 \times 10^{-4}\ \text{cm}^{-1}$ on expanding this interval. The behaviour of three energy levels as a function of ξ was followed (Table I); $n = 56$ corresponds to a level just at the position of the original avoided crossing, $n = 46$ is at the energy of the maximum in

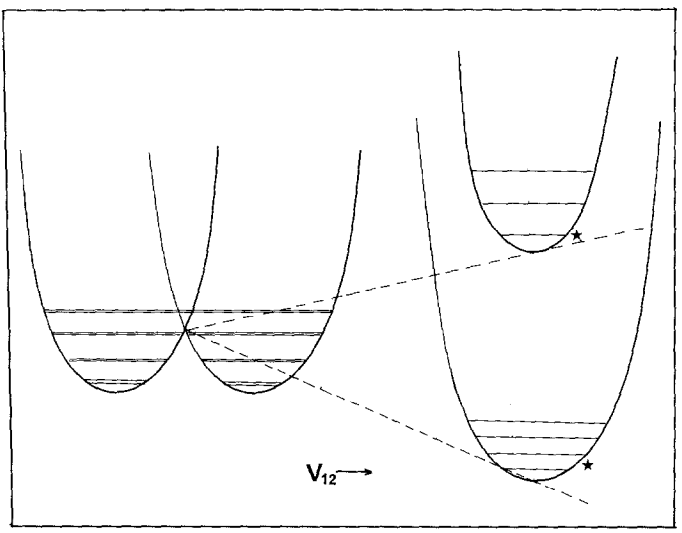

Fig. 1. The two uncoupled parabolic potentials crossing at V_x, are shown schematically on the left and the strongly coupled (adiabatic) states on the right. The strength of coupling, V_{12}, increases from left to right. The locus of the minimum of the upper adiabatic state (that would be obtained by solving the 2 state electronic problem at a given separation) is the linearly rising dashed line, $V_{12} + V_x$. The locus of the barrier maximum in the lower state, which becomes the true minimum when $V_{12} > V_x$, is the lower dashed line $V_x - V_{12}$. In the limit of strong coupling, the wells again become parabolic though the equally spaced energy levels are subject to local perturbations.

TABLE I

The Convergence wth Step Length ξ of Three Eigenvalues in the Coupled State Problem

$\xi * 10^4$/Å	E_{56}/cm^{-1}	E_{46}/cm^{-1}	E_{28}/cm^{-1}
4	4958.280	4019.391	2584.144
5	4958.094	4019.281	2584.092
6	4967.866	4019.147	2584.032
8	4967.288	4018.808	2583.893
10	4966.544	4018.371	2583.709
12	4965.634	4017.837	2583.485
15	4963.958	4016.854	2583.067
20	4960.337	4014.728	2582.167
25	4955.678	4011.992	2581.014
30	4949.978	4008.645	2579.602
a_0	4958.605	4019.581	2584.222
a_1	1.318(+1)	9.173	−4.587(−1)
a_2	−2.074(+6)	−1.218.(+6)	−5.132(+5)
σ	1.6(−3)	1.08(−3)	2.4(−3)

Note. The coefficients of the least squares fit $E_n = a_0 + a_1\xi + a_2\xi^2$ are given below each quantum state, together with the standard deviation, σ, of the fit. The end points of the tabulation were $x_1 = 0$, $x_N = \text{NINT}(3/\xi)$. Thus, for $\xi = 4 \times 10^{-4}$, 7501 grid points were taken in the interval [0, 3]. For those values of ξ not giving an integral number of steps in this interval, the minimum necessary extension to x_N was always $\leqslant 10^{-3}$ Å.

the new adiabatic potential and $n = 29$ is well below the barrier. The levels with $E < 4000\ \text{cm}^{-1}$ are doubled due to tunneling and the splitting $E_{29} - E_{30}$ is $9.85\ \text{cm}^{-1}$. The quadratic convergence is clearly indicated by the least squares fit $E_n(\xi) = a_0 + a_1\xi + a_2\xi^2$, where a_2 is 5–7 orders of magnitude greater than a_1. The increase in a_2 with E_n is simply due to the shortening wavelength of the vibrational motion. For an uncoupled harmonic oscillator the dependence of a_2 on E_n should strictly quadratic, and this is rougly the behaviour displayed in a more extensive survey of coupled systems.

5. A Model Vibronic Coupling Problem

We take the system of coupled states discussed above, but now with the following parameter values: $k = 20{,}000\ \text{cm}^{-1}\ \text{Å}^{-2}$, $\delta = 0.1$ Å, $\mu_{12} = 20$ amu, $V_{12}(x) = V_{12}$. The constant coupling potential is introduced so that the reflection symmetry, $x \leftrightarrow 1 - x$ can be used to unravel the correlation diagram. Whether $V_{12}(x)$ is constant or not makes no difference to the speed of bisection, nor does the functional form of $V_{11}(x)$ and $V_{22}(x)$ though strongly anharmonic potentials would considerably slow up the solution in terms of a harmonic oscillator basis.

Taking this model, our aim is to follow the correlation diagram of, say, the first 20 eigenstates as a function of the strength of coupling V_{12}. The solution of the little 2×2 electronic state coupling problem with constant V_{12} indicates that for large V_{12} (so that the lower adiabatic potential has only a single minimum) the adiabatic eigenstates are again approximately quadratic in the displacement from equilibrium (see Fig. 1) and in these new potentials the two natural frequencies for molecular oscillation are

$$\omega_{1,2}^{(0)} = \{k(1 \pm 2k\delta^2/V_{12})\,\mu^{-1}\}^{1/2}. \tag{12}$$

Thus, as V_{12} increases, the average of the vibrational level spacing $(1/2(\omega_1^{(0)} + \omega_2^{(0)})$ in the two new vibronic manifolds should slowly approach the original spacing in the uncoupled problem. For the parameter values given above, we find for the uncoupled case $\omega^0 = 259.3\ \text{cm}^{-1}$.

The calculations were performed with $N = 800$ and 1200 and the results extrapolated to $\xi = 0$. The uncoupled extrapolated zero point energy agrees with the exact value to 1 part in 10^6. A portion of the complete correlation diagram is shown in Fig. 2. Calculations were performed with $N = 1200$ ($\xi = 0.001$) and, by comparison with extrapolated values, results are accurate to 1 part in 10^4 over the whole diagram. The precision parameter was set to $0.1\ \text{cm}^{-1}$ at the bisection stage, followed by one Newton Raphson interpolation in $\Delta^{(N)}(E)$.

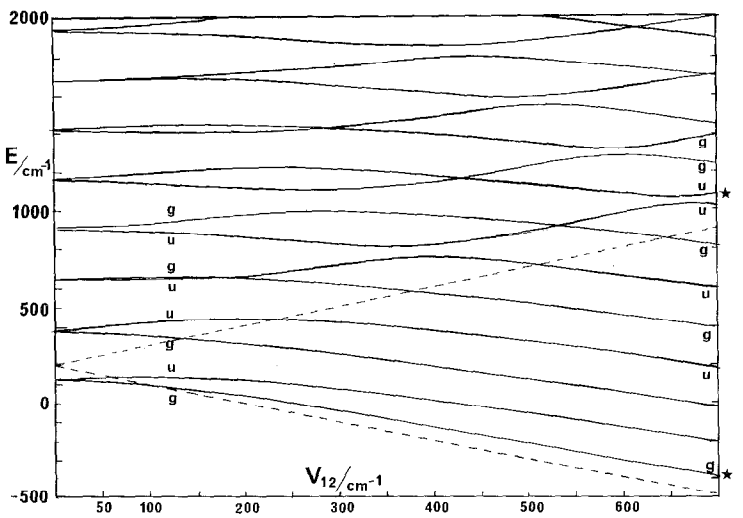

FIG. 2. The correlation diagram of the first 16 energy levels for the potentials and coupling term defined in Section 5 and qualitatively shown in Fig. 1, but with a lower barrier ($V_x = 200\ \text{cm}^{-1}$) lying between the $v = 0$ and $v = 1$ doublets. The small splitting at the left is characteristic of the slightly perturbed diabatic states, followed by an intermediate coupling region. At the right, two sets of nearly adiabatic vibronic levels have energed. Those falling with increasing V_{12} are associated with the lower adiabatic electronic state and the rising curves belong to the upper adiabatic state. The dashed lines are the loci of the minima of the two adiabatic states as in Fig. 1. The starred states correspond to the zero point motion of Fig. 1.

The correlation diagram is displayed in Fig. 2. It shows clearly the evolution of the vibronic levels characteristic of the two adiabatic states from the uncoupled ones ($V_{12}=0$). Thus starting from the left, the first three doublets evolve into the first six levels of the lower adiabatic state. Then in the higher doublets one member evolves into a level of the upper adiabatic state and its partner into a member of the lower state adiabatic state.

Several avoided and unavoided crossings are visible. With regard to the symmetry classification, we take as the symmetry operator ($x \leftrightarrow -x$) and this has the effect of transforming V_{11} into V_{22} (and leaving V_{12} unchanged). Applying this operator to the coupled wave equation (2) leads to the requirement

$$\phi_{1,2}(-x) = \pm \phi_{2,1}(x)$$

and these two possibilities must be called g and u. Somewhat perversely, this leads to the lowest vibrational state of the upper adiabatic electronic state being classified u. The explanation is simply that this electronic state is itself odd with respect to interchange of the nuclear positions (it is an anti-symmetric combination $\psi_1 - \psi_2$ of the original diabatic states). Note also the reversal of the order of the g/u pairs for small V_{12} as the energy increases. For the third pair of levels the splitting remains almost zero until $V_{12} \sim 250\ \mathrm{cm}^{-1}$ (and passes through zero at $V_{12} \sim 150\ \mathrm{cm}^{-1}$). The reason is that the 1st order perturbed energy splitting, given by

$$\begin{aligned} \delta E_n^{(1)} &= \tfrac{1}{2} V_{12} \left[\int_{-\infty}^{\infty} (\phi_{1n}^{(0)} + \phi_{2n}^{(0)})^2 \, dx - \int_{-\infty}^{\infty} (\phi_{1n}^{(0)} - \phi_{2n}^{(0)})^2 \, dx \right] \\ &= 2V_{12} \int_{-\infty}^{\infty} \phi_{1n}^{(0)} \phi_{2n}^{(0)} \, dx \end{aligned} \tag{13}$$

can be either positive or negative depending on the phase of the uncoupled vibrational functions $\phi_{1n}^{(0)}$ and $\phi_{2n}^{(0)}$ in the overlap region. At $n=3$ the overlap is almost zero and for the next few pairs of levels the u state lies lower until another reversal occurs.

The adiabatic picture is not established until the coupling is rougly twice that of the diabatic state vibrational spacing (or twice the larger of $\omega_1^{(0)}$ and $\omega_2^{(0)}$ if the two potential wells have different force constants). In terms of the adiabaticity parameter $\gamma = V_{12}/\hbar\omega^{(0)}$ introduced by Dressler [7], the strong coupling regime begins when $\gamma \gtrsim 2$.

5. Conclusions

The methods of numerically evaluating the Sturm sequence to find the roots of a tridiagonal matrix can be adapted to the pentadiagonal case. All two state coupling

eigenvalue problems can then be solved by this technique which, we suggest, should be the preferred one for this class of problem. In particular, we have illustrated its use in a vibronic coupling problem in a diabatic basis up to the 56th level and the method works equally well for bands of high or low rovibrational levels. Extrapolation with respect to the grid spacing (ξ) is smooth. Judging from the model calculations presented, the behaviour of the λ-determinant Sturm sequence in the single channel double minimum potential problem, tunnelling through classically forbidden regions offers no difficulty.

The disadvantages of the determinantal method are: (1) convergence with respect to ξ is quadratic compared with ξ^4 in Numerov based methods; (2) although the basic algorithms are simple to write down for n coupled equations, the number of recursive steps increases as 2^n. We have successfully used the method for $n=3$, but four coupled states may be the practicable limit.

The advantages are: (1) the transparency of the method; (2) its speed, arising from the simplicity of the algorithm and the fact that the matching procedure in the integration methods is avoided; (3) its stability in barrier penetration problems.

Appendix A

The particular structure of the discretized Hamiltonian matrix for the two state coupling problem (Eq. (2)) is, in reduced form (assuming $\phi_0^{(1)}$ and $\phi_0^{(2)}$ to be zero),

$$\begin{bmatrix} \alpha_1-\lambda & \gamma_1 & -1 & \cdot & \cdot & \cdot & 0 \\ \gamma_1 & \beta_1-\lambda & 0 & -1 & & & \cdot \\ -1 & 0 & \alpha_2-\lambda & \gamma_2 & -1 & & \cdot \\ 0 & -1 & \gamma_2 & \beta_2-\lambda & 0 & -1 & \cdot \\ 0 & 0 & -1 & 0 & \alpha_3-\lambda & \gamma_3 & \cdot \\ \vdots & & & & & \ddots & \\ 0 & \cdot & \cdot & -1 & \gamma_N & & \beta_N-\lambda \end{bmatrix}, \tag{A1}$$

where α_i is the value of the lower state diabatic Hamiltonian (in reduced units) evaluated at the ith mesh point, β_i the corresponding value in the upper state and γ_i the reduced value of the coupling function V_{12} at x_i,

$$\begin{aligned} \alpha_i &= (2\mu\xi^2/\hbar^2)\, V_{11}(x_i)+2 \\ \gamma_i &= (2\mu\xi^2/\hbar^2)\, V_{12}(x_i) \\ \lambda &= 2\mu\xi^2 E/\hbar^2. \end{aligned} \tag{A2}$$

There are two sorts of minor determinant of increasing order down the principal diagonal: those terminating in $\alpha_i-\lambda$ and in $\beta_i-\lambda$. (The order of the latter will necessarily be one greater than that of the former). We denote these two minors by

$A^{(i)}$ and $B^{(i)}$ [$B^{(2)}$ and $A^{(3)}$ are outlined in (A1)]. Then, with the aid of two further minors of $B^{(i)}$,

$$\begin{aligned} G^{(i)} &= B^{(i)}_{i,i-1} \\ H^{(i)} &= -B^{(i)}_{i,i-2}. \end{aligned} \tag{A3}$$

We have the following recursion relations for the sequence (9), with $A^{(1)} \cdots A^{(i)}$, $B^{(i)}$, $A^{(i+1)}$, $B^{(i+1)} \cdots B^{(N)}$ constituting a Sturm sequence,

$$\begin{aligned} A^{(i)} &= (\alpha_i - \lambda)\, B^{(i-1)} - (\beta_{i-1} - \lambda)\, B^{(i-2)} + A^{(i-2)} \\ B^{(i)} &= (\beta_i - \lambda)\, A^{(i)} - \gamma_i G^{(i)} + H^{(i)} \\ G^{(i)} &= \gamma_i\, B^{(i-1)} + G^{(i-1)} \\ H^{(i)} &= B^{(i-2)} - \gamma_i G^{(i-1)} - (\alpha_i - \lambda)\, A^{(i-1)}. \end{aligned} \tag{A4}$$

The sign changes in the Sturm sequence are then counted by the number of negative values of the successive ratios $A^{(i)}/B^{(i-1)}$ and $B^{(i)}/A^{(i)}$ in scanning i from 1 to N. The actual algorithm uses the auxiliary ratios

$$\begin{aligned} S1_i &= B^{(i)}/A^{(i)} \\ S2_i &= A^{(i)}/B^{(i-1)} \\ S3_i &= A^{(i)}/A^{(i-1)} \\ S4_i &= G^{(i)}/A^{(i)} \\ S5_i &= H^{(i)}/A^{(i)} \end{aligned} \tag{A5}$$

and their reciprocals $RN_i = 1/SN_i$, etc. The recursive sequence for ratios is then, in order of execution,

$$\begin{aligned} S2_i &= (\alpha_i - \lambda) - ((\beta_{i-1} - \lambda) * R2_{i-1} - R3_{i-3}) * R1_{i-1} \\ R3_i &= R1_{i-1} * R2_i \\ S4_i &= \gamma_i * R2_i + S4_{i-1} * R3_i \\ S5_i &= (R2_{i-1} - \gamma_i * S4_{i-1} - (\alpha_i - \lambda)) * R3_i \\ S1_i &= (\beta_i - \lambda) - \gamma_i * S4_i + S5_i \end{aligned}$$

and the initial values are

$$\begin{aligned} S1_1 &= ((\alpha_1 - \lambda)(\beta_1 - \lambda) - \gamma_1^2)/(\alpha_1 - \lambda) = 1/R_1 \\ R3_1 &= 0 \\ S4_1 &= \gamma_1/(\alpha_1 - \lambda). \end{aligned}$$

If the Lth root is required, the value of λ is refined by bisection between successively closer values, $\lambda_<$ and $\lambda_>$ that give L and $L-1$ sign changes respectively in the Sturm sequence. The process is stopped when $\lambda_<$ and $\lambda_>$ differ by less than a preset limit η.

This bisection can be the most inefficient part of the whole scheme. The more efficient Newton Raphson (NR) interpolation cannot be used on the nearly discontinuous ratio function $S_N(\lambda)$, but we have found that the NR procedure works well on the determinant $B^{(N)}(\lambda)$ itself. ($\Delta^{(N)}$ in the notation of Section 2). At first sight this is a rather hazardous procedure because the full determinant (unless λ is very close to a root) will typically have a magnitude in excess of 10^{34}. However, we have found good linear behaviour in the vicinity of a root once λ_L has been located to roughly 10^{-3} of the adjacent root separation. In order to avoid possible real overflow in evaluating $B^{(N)}$, the starting values for the Sturm sequence (A4) (i.e., $A^{(1)}$, $B^{(1)}$, $G^{(1)}$, and $B^{(0)}$ $(=1)$ are all scaled by 10^{-20} before the sequence is generated in the usual way. The sequence itself should not begin too far inside the classical turning point.

To summarise, then. A root is located with a precision $10^{-3}\lambda_L$ by bisection. This might take 5 to 6 passes through the Sturm sequence. An NR search for the zero of $B^{(N)}(\lambda)$ is then made in the interval $(\lambda<, \lambda>)$. This will take 2, or just possibly 3 passes through the slightly faster Sturm sequence (A4) to achieve a precision of 10^{-5} or better in λ_L.

Appendix B

We show that the single channel eigenvalue problem with the second order differential operator correct to $O(\xi^4)$ gives rise to a pentadiagonal λ-matrix.

The central difference formula for $d^2\phi/dx^2$ to $O(\xi^4)$ is

$$\phi_i'' = \frac{1}{12\xi^2}(-\phi_{i-2} + 16\phi_{i-1} - 30\phi_i + 16\phi_{i+1} - \phi_{i+2}) + \frac{\xi^4}{90}\phi^{(vi)}. \tag{B1}$$

Provided both ϕ_{-1} and ϕ_0 are zero (the boundary condition appropriate to the regular solution in a classically forbidden region), the single channel one-dimensional wave equation then becomes, in discretized form,

$$\begin{bmatrix} \alpha_1-\lambda & 16 & -1 & 0 & \cdot & 0 \\ 16 & \alpha_2-\lambda & 16 & -1 & 0 & \cdot \\ -1 & 16 & \alpha_3-\lambda & 16 & -1 & \cdot \\ 0 & & & \cdot & & \cdot \\ \cdot & & & & \cdot & \cdot \\ 0 & \cdot & \cdot & -1 & 16 & \alpha_N-\lambda \end{bmatrix} \begin{bmatrix} \phi_1 \\ \phi_2 \\ \cdot \\ \cdot \\ \cdot \\ \phi_N \end{bmatrix} = 0, \tag{B2}$$

where

$$\alpha_i = (2\mu/\hbar^2)\,\xi^2 V_i - 30, \qquad \lambda = 2\mu\xi^2 E/\hbar^2.$$

The Hamiltonian λ-matrix is thus pentadiagonal, with constant off-diagonal entries. Finding the eigenvalues thus involves the same type of Sturm sequence as discussed in Appendix A, but is quicker to execute. We have only one type of principal minor, $A^{(i)}$ ($\equiv \Delta^{(i)}$), and two further minors, $G_i = \Delta^{(i)}_{i,i-1}$ and $H_i = \Delta^{(i)}_{i,i-2}$,

$$\begin{aligned} G_i &= 16A_{i-1} + G_{i-1} \\ H_i &= -16G_{i-1} - (\alpha_i - \lambda)\, A_{i-2} + A_{i-3} \\ A_i &= (\alpha_i - \lambda)\, A_{i-1} - 16G_{i-1} - H_{i-1}, \end{aligned} \tag{B3}$$

and the recursion is started by $A_{-1} = 0$, $A_0 = 1$, $A_1 = \alpha_1 - \lambda$, $G_0 = 0$. The Numerov recursion formula is rather simpler

$$\phi_{i+1} = \frac{\phi_i(2 + (10/12)\,\xi^2(\alpha_i - \lambda)) - \phi_{i-1}(1 - (1/12)(\alpha_i - \lambda)\,\xi^2)}{1 - (1/12)\,\xi^2(\alpha_{i+1} - \lambda)}. \tag{B4}$$

The discretized wave function ϕ_i (in the single channel one-dimensional case only) forms a Sturm sequence, so we can find eigenvalues by bisection in the sequence

$$\phi_1(\lambda), \phi_2(\lambda), \phi_3(\lambda), \ldots, \phi_N(\lambda)$$

from the number of negative values of

$$S_{i+1} = \frac{\phi_{i+1}}{\phi_i} = \frac{(2 + (10/12)\,\xi^2(\alpha_i - \lambda)) + R_i(1 - (1/12)\,\xi^2(\alpha_{i-1} - \lambda))}{1 - (1/12)\,\xi^2(\alpha_{i+1} - \lambda)} \tag{B5}$$

(where $R_i = 1/S_i$). This might seem preferable to the slightly longer sequence (B3). For potentials with a single minimum, the two methods are completely concordant, with the Numerov technique (B5) yielding the higher accuracy because of the smaller remainder term $\frac{1}{240}\,\xi^4\phi^{(vi)}$. However, for double minimum problems involving states below the top of the potential barrier (e.g., inversion doublet splitting) the Numerov method is unstable in the classically forbidden regions. This results in an inability to resolve nearly degenerate levels. We have used the sequence (B3) (and the simpler tridiagonal one based on $\delta^{(2)}$ alone) with complete success in many internal rotation and inversion problems with splittings down to $10^{-3}\,\mathrm{cm}^{-1}$.

Appendix C

The vibronic two state coupling problem in an adiabatic basis is often reduced to the coupled equations (see, e.g., Ref.[8]),

$$\begin{aligned} (-(\hbar^2/2\mu)\,d^2/dx^2 + V_{11}(x) - E)\,\phi_1(x) &= T_{12}(x)\,d\phi_2/dx \\ (-(\hbar^2/2\mu)\,d^2/dx^2 + V_{22}(x) - E)\,\phi_2(x) &= -T_{12}(x)\,d\phi_1/dx. \end{aligned} \tag{C1}$$

If the second order central difference operator is substituted for d^2/dx^2 and if the coupling amplitude function $R_{12}(x)$ is constant, we have

$$\begin{bmatrix} \alpha_1-\lambda & \gamma & -1 & 0 & \cdot & 0 \\ \gamma & \beta_1-\gamma & -\gamma & -1 & \cdot & \cdot \\ -1 & -\gamma & \alpha_2-\lambda & \gamma & -1 & \cdot \\ 0 & & & & & \cdot \\ \vdots & & & & \ddots & \vdots \\ 0 & \cdot & -1 & \gamma & & \beta_N-\lambda \end{bmatrix} \begin{bmatrix} \phi_1^{(1)} \\ \phi_{3/2}^{(2)} \\ \phi_2^{(1)} \\ \cdot \\ \vdots \\ \phi_{N+1/2}^2 \end{bmatrix} = 0, \qquad \text{(C2)}$$

where

$$\alpha_i = (2\mu/\hbar^2)\,\xi^2 V_{11}(x_i) + 2$$
$$\beta_i = (2\mu/\hbar^2)\,\xi^2 V_{22}(x_i) + 2$$
$$\gamma = 2\mu\xi T_{12}/\hbar^2.$$

Note that the second part of the vibrational wave function, $\phi_{i+1/2}^{(2)}$ is tabulated at points midway between the adjacent $\phi^{(1)}$ values, $\phi_i^{(1)}$ and $\phi_{i+1}^{(1)}$. This allows the more accurate central difference formula (with error $-\frac{1}{24}\xi^2\phi'''$).

$$\phi_i' = \frac{1}{\xi}(\phi_{i-1/2} - \phi_{i+1/2}) \qquad \text{(C3)}$$

to be used for the first order differential operator.

The Sturm sequence is principal minors of the λ-determinant from (C2) is developed from Eq. (9) and root finding proceeds as described in Appendix A, beginning with bisection.

In practice (see, for e.g., [9]), $T_{12}(x)$ may be a rather sharply varying function of the vibrational coordinate near an avoided crossing and the tabular positions of γ_i have to be decided. The Hermitian nature of **H** must be retained and it turns out that the correct positioning of $\{\gamma\}$ is midway between x_i and $x_i + 1/2$,

$$\gamma_{1/4}, \gamma_{3/4} \cdots \gamma_{i-1/4}\gamma_{i+1/4} \cdots \gamma_{N+1/4}.$$

We are investigating the accuracy and stability of the Sturm sequence method for this problem.

References

1. A. U. Hazi and H. S. Taylor, *Phys. Rev. A* **1** (1970), 1109.
2. K. P. Lawley and R. Wheeler, *J. Chem. Soc., Faraday Trans.* 2 **77** (1981), 1133.
3. B. R. Johnson, *J. Chem. Phys.* **69** (1978), 4678.
4. O. Atabek and R. Lefebvre, *Chem. Phys.* **52** (1980), 199.

5. J. H. WILKINSON, "The Algebraic Eigenvalue Problem, Oxford Univ. Press (Clarendon), 1965, p.302.
6. T. MUIR AND W. H. METZLER, "A Treatise on the Theory of Determinants" (privately published, Albany, N.Y., 1930), p. 615.
7. K. DRESSLER, "Photophysics and Photochemistry above 6 eV," Edited by F. Lacmani (Elsevier, Amsterdam, 1985), p. 327.
8. D. STAHEL, M. LEONI AND K. DRESSLER *J. Chem. Phys.* **79** (1983), 2541.
9. K. DRESSLER, R. GALLUSSER, P. QUADRELLI, AND L. WOLNIEWICZ, *J. Mol. Spectros.* **75** (1979), 205.